JOURNAL OF APPLIED ELECTROCHEMISTRY 2 (1972) 83–90

A mathematical model for platinum/PTFE/porous nickel fuel cell oxygen diffusion electrodes

P. D. POWER* and M. J. R. ADAMS†

Received 5 May 1971

This paper describes the cylindrical agglomerate model for oxygen/alkali gas diffusion electrodes fabricated from platinum, PTFE and porous nickel. Corrections for the increase in hydroxyl ion concentration with increasing current density have been made to the original model of Brown and Horve. Changes in performance by variation of the bulk structural parameters, e.g. agglomerate radius, porosity and tortuosity, have been studied. Theoretical modes of electrode decay have been explored.

Introduction

Mathematical models have been proposed for many different types of fuel cell electrodes. The work up to 1966 has been extensively reviewed by de Levie [1]. More recently various models have been proposed for catalyst—PTFE electrodes. This type of electrode can be prepared by applying a suspension of catalyst and PTFE to a porous metal or a metal screen substrate. Austin and Almaula [2] posed a simple pore type model, where only a thin layer at the catalyst surface is wetted by the electrolyte and can take part in the electrode reaction. However, a comparison of electrochemical and BET surface area measurements shows that the catalyst is completely wetted. A model assuming wetted spherical catalyst agglomerates surrounded by a non-wetted PTFE phase was put forward by Brown [3]. This model did not consider the IR drop within the catalyst structure and was improved upon by Horve [4] and Giner and Hunter [5]. These workers considered the catalyst to be in the form of wetted cylindrical agglomerates. The present work considers a specific reaction, the oxygen reduction on platinum, in potassium hydroxide, in terms of this original model and an improved model. The reasons for carrying out this work were firstly, to predict electrode performance under different operating conditions and to quantitatively compare electrodes prepared by different procedures; secondly, to determine bulk parameters for the electrode structure, such as porosity, tortuosity and agglomerate radius, and thirdly, to investigate the relative importance and nature of the different processes contributing to the observed decay in performance. The work described below is mainly concerned with the theoretical aspects of fuel cell performance as is suggested by the title of the paper.

Theoretical development of model

The cylindrical agglomerate model considers the catalyst to consist of cylindrical platinum/electrolyte agglomerates (Figs. 1 and 2) separated from the PTFE/gas phase by a thin film of electrolyte [5]. When current is flowing there will be a radial oxygen concentration gradient and an axial potential gradient throughout the agglomerate. The oxygen concentration can be determined as

* Present address: Unilever Ltd, London.
† Present address: 3M Co. Ltd.

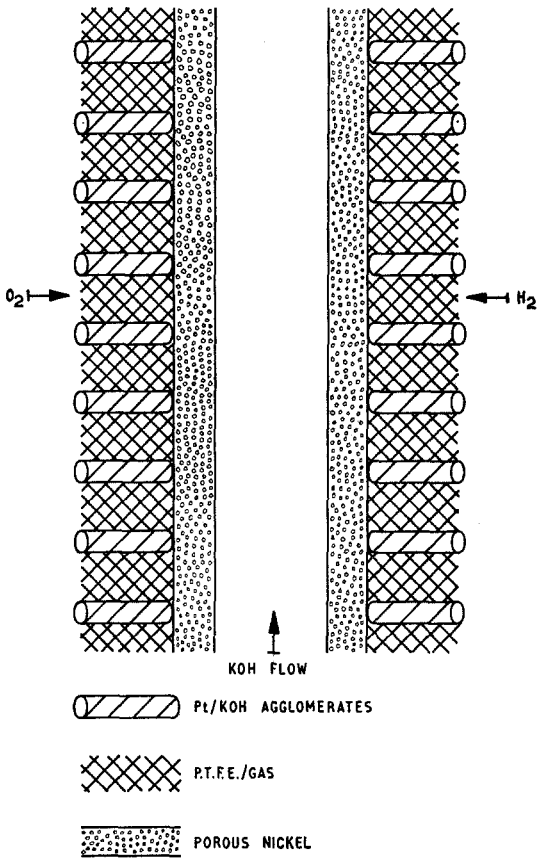

Fig. 1. Schematic representation of the theoretical fuel cell.

a function of the radius by solving Fick's second law for diffusion through the film [1] and through the agglomerate [2].

$$\frac{d^2C}{dr^2} + \frac{D}{r}\frac{dC}{dr} = 0 \qquad (1)$$

with boundary conditions,

$$C = C_0 \text{ at } r = R+\delta$$

and

$$C = C_2^0 \text{ at } r = R$$

$$\frac{d^2C}{dr^2} + \frac{D\theta}{r\tau_r}\frac{dC}{dr} - KC = 0 \qquad (2)$$

with boundary conditions.

$$dC/dr = 0 \text{ at } r = 0$$

and

$$C = C_2^0 \text{ at } r = R.$$

KC represents the removal of oxygen by reduction and allows for the presence of the platinum particles in the diffusion path.

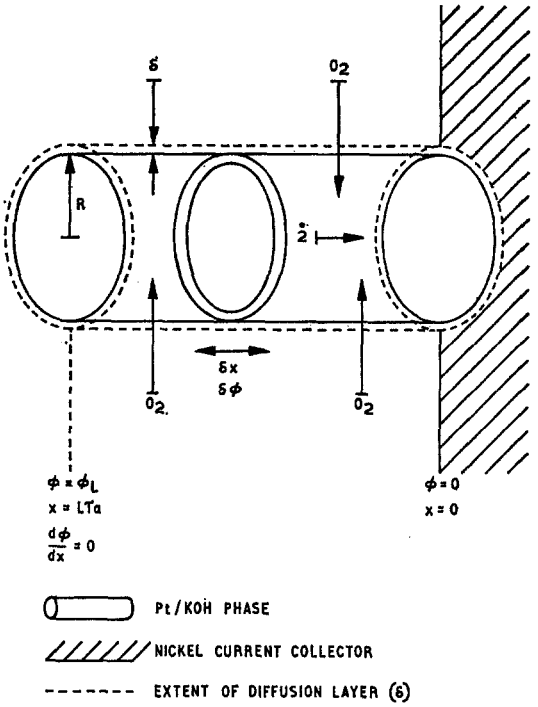

Fig. 2. A cylindrical agglomerate, showing the assumed direction of oxygen diffusion and the extent of the diffusion layer (δ).

The local current density is given by

$$j = j_0 \frac{C}{C_0}\exp\left(\frac{\alpha\, NF}{R_0T}(E-\phi)\right). \qquad (3)$$

Hence

$$K = \frac{S_g\rho(1-\theta)j_0}{NFC_0}\exp\left(\frac{\alpha\, NF}{R_0T}(E-\phi)\right) \qquad (4)$$

where $S\rho_g(1-\theta)$ is the surface area term.

From Ohm's law the current per agglomerate is given by

$$i_a = \frac{\sigma m \Pi R^2\theta}{\tau_r}\left(\frac{d\phi}{dx}\right)_{x=0} \qquad (5)$$

N_a, the number of agglomerates per cm^2 of electrode, can be calculated from the loading W, i.e.

$$N_a = \frac{W}{\Pi R^2 L\tau_a\rho(1-\theta)}. \qquad (6)$$

The total current density is

$$i = \frac{W\theta}{\tau_a\tau_r L\rho(1-\theta)}\left(\frac{d\phi}{dx}\right)_{x=0} \qquad (7)$$

The problem is the determination of

$$\left(\frac{d\phi}{dx}\right)_{x=0}.$$

Equations (1) and (2) can be solved to give C_j, the concentration at the surface of the cylinder. The local current density on the surface can be obtained by substitution into equation (3), and is related to the current in the axial direction by the equation

$$\frac{di}{dx} = 2\Pi R_j. \tag{8}$$

The axial current is given by Equation (9) using Ohm's law.

$$i = \frac{\Pi R^2 \theta}{\tau_r}\frac{d\phi}{dx}, \tag{9}$$

hence

$$\frac{d^2\phi}{dx^2} = -\frac{\sigma m \theta R_j}{2\tau_r}. \tag{10}$$

Substituting for the local current density, j, gives expression (11)

$$\frac{d^2\phi}{dx^2} = -\frac{K_2 \exp(B(E-\phi))}{f(E-\phi)+K_3\exp(B(E-\phi))} \tag{11}$$

where

$$B = \frac{\alpha\, NF}{R_0 T} \tag{12}$$

$$K_2 = \frac{S_g\rho(1-\theta)j_0\tau_r}{\sigma m\theta} \tag{13}$$

$$K_3 = \frac{R^2 \log_e\left(1+\frac{\delta}{R}\right)S_g\rho(1-\theta)j_0}{2NF\,D_{O_2}S_{O_2}} \tag{14}$$

$$f(E-\phi) = \frac{K_4}{2}\frac{I_0(K_4)}{I_1(K_4)} \tag{15}$$

$$K_4^2 = \frac{R^2 S_g\rho(1-\theta)j_0\tau_r}{NFD_{O_2}S_{O_2}\theta}. \tag{16}$$

The numerator in Equation (11) is the activation polarization term whereas the left-hand denominator term, involving the Bessel function ratio, represents diffusion polarization in the agglomerate and the right-hand denominator term represents diffusion through the thin film δ.

The solution of Equation (11) is difficult because the boundary conditions for the first integration involve ϕ_L (the potential drop at $x = L\tau_a$) which is unknown and can only be obtained by a further integration.

The approach that has been adopted in the present work is to consider two polarization regions. The first is where $\phi \ll E$. In this case the integration of (11) is with respect to x and $\left(\frac{d\phi}{dx}\right)_{x=0}$ can be easily obtained.

The second region is where the Bessel function ratio $\frac{I_0(K_4)}{I_1(K_4)}$ tends to unity. Equation (11) becomes:

$$\frac{d^2\phi}{dx^2} = -\frac{K_2\exp(B(E-\phi))}{K_5\exp\left(\frac{B}{2}(E-\phi)\right)+K_3\exp(B(E-\phi))} \tag{17}$$

where

$$K_5 = \frac{1}{2}\left(\frac{R^2 S_g\rho(1-\theta)j_0\tau_r}{NFD_{O_2}S_{O_2}\theta}\right)^{\frac{1}{2}}. \tag{18}$$

Equation (17) can be solved analytically using the boundary conditions

$$\phi = 0 \text{ at } x = 0 \text{ and } \frac{d\phi}{dx} = 0 \text{ at } x = L\tau_a$$

to give

$$\left(\frac{d\phi}{dx}\right)_{x=0} = K_7\left[\log_e\left\{1+K_6\exp\left(\frac{BE}{2}\right)\right\} - \log_e\{1+K_6\exp(B(E-\phi_L))\}\right]^{\frac{1}{2}} \tag{19}$$

where

$$K_7 = \left(\frac{2K_2}{BK_3}\right)^{\frac{1}{2}} \tag{20}$$

and

$$K_6 = \frac{K_3}{K_5}. \tag{21}$$

However ϕ_L is unknown, but may be obtained by integrating $\left(\frac{dx}{d\phi}\right)$ which is given by

$$\frac{dx}{d\phi} = \frac{1}{K_7}\left[\log_e\left\{1+K_6\exp\left(\frac{B}{2}(E-\phi)\right)\right\} - \log_e\left\{1+K_6\exp\left(\frac{B}{2}(E-\phi_L)\right)\right\}\right]^{-\frac{1}{2}} \tag{22}$$

i.e.

$$L\tau_a = \frac{1}{K_7}\int_0^{\phi L}\left[\log_e\left\{1+K_6\exp\left(\frac{B}{2}(E-\phi)\right)\right\} - \log_e\left\{1+K_6\exp\left(\frac{B}{2}(E-\phi_L)\right)\right\}\right]^{-\frac{1}{2}} d\phi. \quad (23)$$

The procedure for the solution is as follows. Equation (23) is integrated numerically using Simpson's method. A value of ϕ_L is guessed and the resulting value of $L\tau_a$ is compared with the known value (note: the integration limit must be slightly less than ϕ_L because the function tends to infinity). From the difference a new value of ϕ_L is calculated and the procedure is repeated until the $L\tau_a$ values agree within a predetermined limit. The calculated value of ϕ_L is substituted into Equation (19) to give $\left(\frac{d\phi}{dx}\right)_{x=0}$ and hence the current density.

In practice it is found that the two polarization regions mentioned above overlap, and a computer program has been written to give the complete current-voltage profile.

The following assumptions have been made in the above analysis:

(a) The agglomerates are cylindrical, not interconnected and of constant radius. The model has been improved to consider a normal distribution of radii. It has been found that the performance is only slightly lower over the whole voltage range as long as the standard deviation is not too large compared to the mean radius (i.e. <30%).

(b) The catalyst particles are flooded with electrolyte and are interconnected with the current collector and other particles. The validity of this assumption is shown by the agreement of the BET surface area of the catalyst and the electrochemical surface area (hydrogen adsorption).

(c) The electronic IR drop within the catalyst is negligible. This assumption can be shown to be reasonable by considering the porosity and the conductivities of platinum and potassium hydroxide.

(d) There are no kinetic or transport limitations in the gas phase. There is no convection within the agglomerates.

(e) The 'Tafel parameters' for the electrode reaction do not depend on the electrode poten-

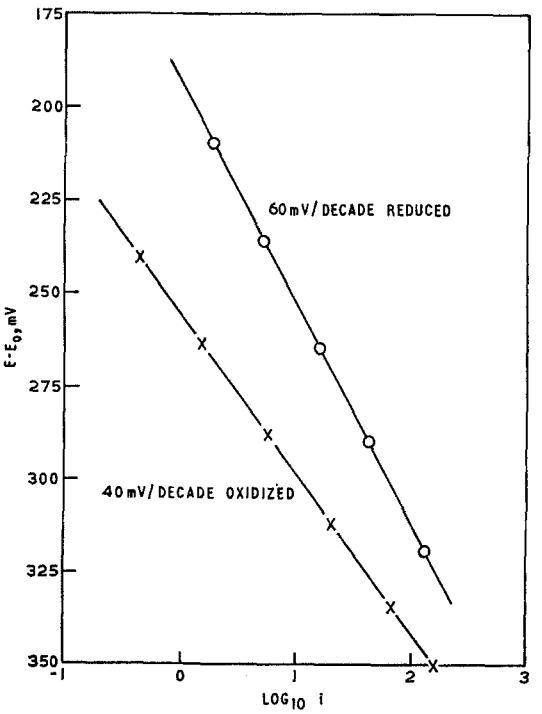

Fig. 3. The experimental Tafel slope variation for oxygen reduction on oxidized and reduced Pt/PTFE electrode.

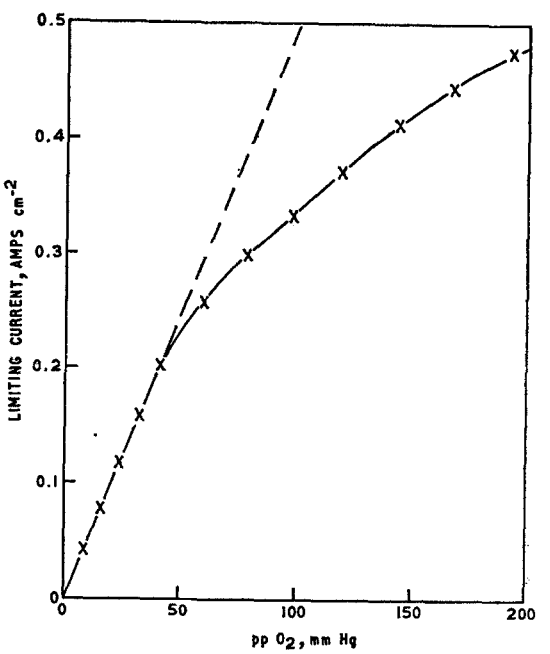

Fig. 4. The experimental variation of the limiting current with partial pressure of oxygen.

tial. It has been shown (Fig. 3) that the 'Tafel parameters' do in fact vary with the oxide/oxygen surface coverage and hence the potential. Although this variation is significant in the Tafel region, it is relatively small at higher current densities.

(f) The electrolyte concentration remains constant.

This is not true at high current densities, OH^- is generated by the half cell reaction:

$$O_2 + 2H_2O + 4e \rightleftharpoons 4OH^- \qquad (24)$$

and although migration and diffusion tend to oppose any concentration build-up, a steady state concentration is reached which depends upon the current and the diffusion barrier presented by the catalyst and the porous nickel substrate. This effect can be best seen by observing the experimental variation of limiting current with oxygen partial pressure (Fig. 4). At low partial pressures, the limiting current is proportional to oxygen solubility and hence partial pressure. The deviation from linearity at higher partial pressures is caused by the decrease in the oxygen solubility and diffusion coefficient with the increasing local OH^- concentration. It has been found that the value of the product D_{O_2} S_{O_2}, calculated for the limiting current on 100% oxygen is about one third of the value that would be observed if no OH^- were formed. This corresponds to a local OH^- concentration of about 7M. An empirical relationship can be derived relating the product D_{O_2} S_{O_2} to the current density based on the results described above. The product D_{O_2} S_{O_2} would be expected to vary approximately with the square of the current. The reason for this is that the effective reaction volume decreases with increasing current density. Empirical relationships have also been derived from experimental data relating the 'exchange current density' and the 'Tafel slope' to the current density to the power $\frac{3}{2}$.

This correction has been introduced into the modified model by correcting the D_{O_2} S_{O_2} product and the Tafel parameters at any given polarization with the current calculated at a slightly lower polarization. This procedure is repeated over the whole current-voltage profile.

Results and discussion

The theoretical current-voltage curves that follow are applicable, unless stated otherwise, to an electrode reaction with the following characteristics.

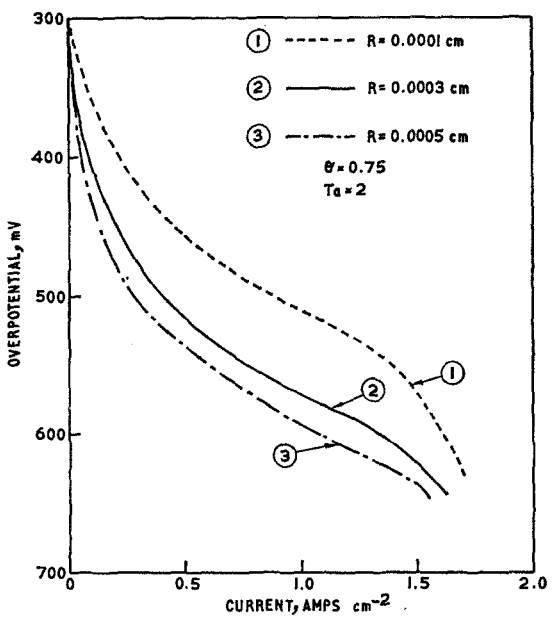

Fig. 5. The theoretical variation of current-voltage curves with agglomerate radius.

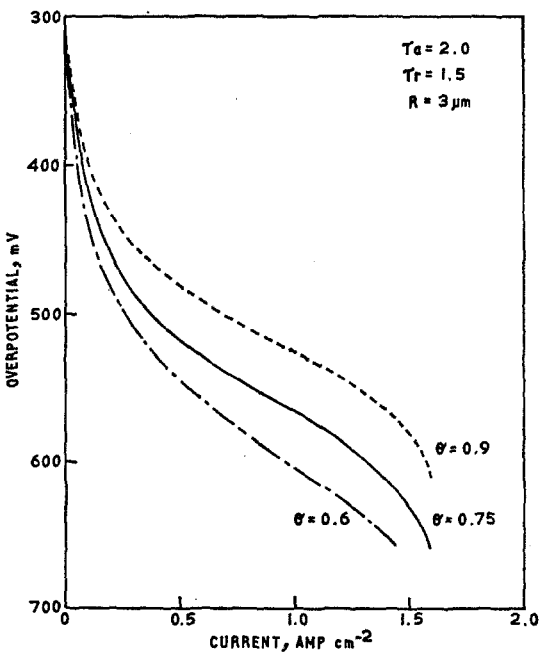

Fig. 6. The theoretical variation of current-voltage curves with agglomerate porosity.

Temperature = 25°C
Exchange current density for O_2 reduction = 10^{-10} A, cm^{-2} (j_0)
Surface area/g platinum (S_g) = 22 m^2g^{-1}
Radial tortuosity (τ_r) = 1·5
Limiting current on O_2 at 0·01 atm = 0·52 A cm^{-2}
Electrolyte conductivity = 0·59 $(ohm\ cm)^{-1}$.

Fig. 5 shows the effect of the variation of agglomerate radius. It can be seen that if the radius could be decreased from 3 μm to 1 μm the performance would double.

Fig. 6 shows the current-voltage curves at three different porosities. The effect on the performance level is again very large.

Variation of the axial tortuosity is shown in Fig. 7. Differences in performance are small at low current densities but become increasingly important at higher values.

Fig. 8 shows the performance profile for an electrode with a normal distribution of radii with a 3 μm mean. It can be seen that with a standard deviation of 1 μm, i.e. 95% of the agglomerates having a radius between 1 and 5 μm, the current voltage is very similar to the curve for the fixed radius.

The effect of a decreased surface area (×0·5)

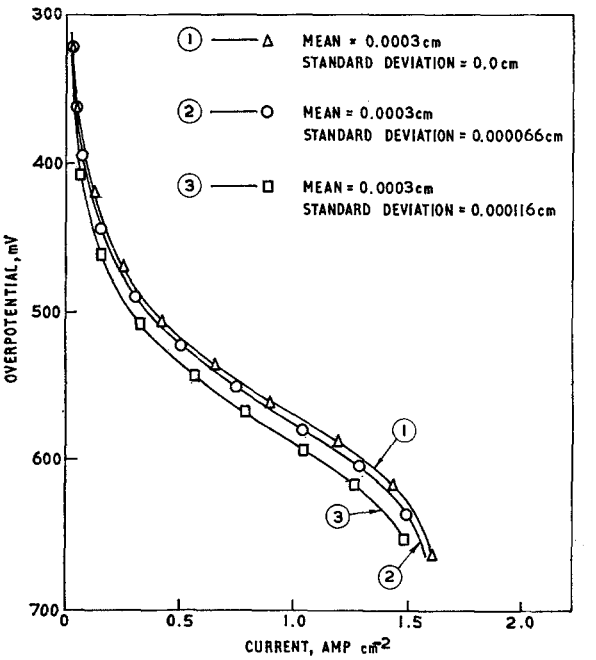

Fig. 8. A comparison of theoretical current-voltage curves for different standard deviations of the agglomerate radius (normally distributed).

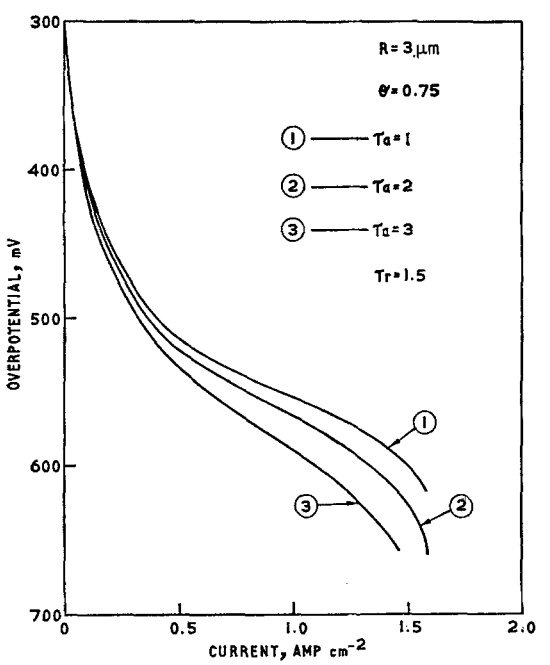

Fig. 7. The theoretical variation of current-voltage curves with axial tortuosity.

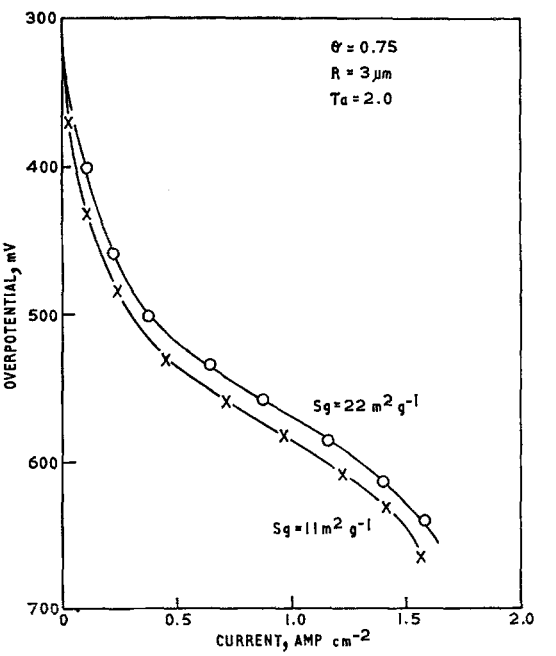

Fig. 9. The effect on a theoretical current-voltage curve of halving the surface area.

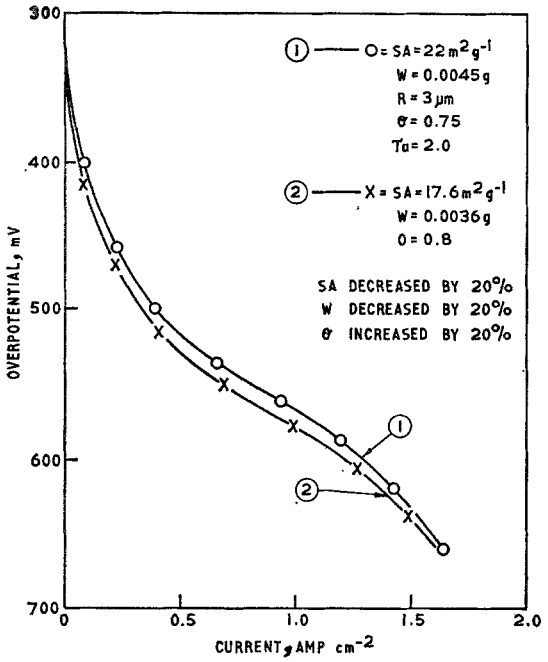

Fig. 10. The theoretical effect of platinum dissolution allowing for a decrease in surface area and loading and an increase in porosity.

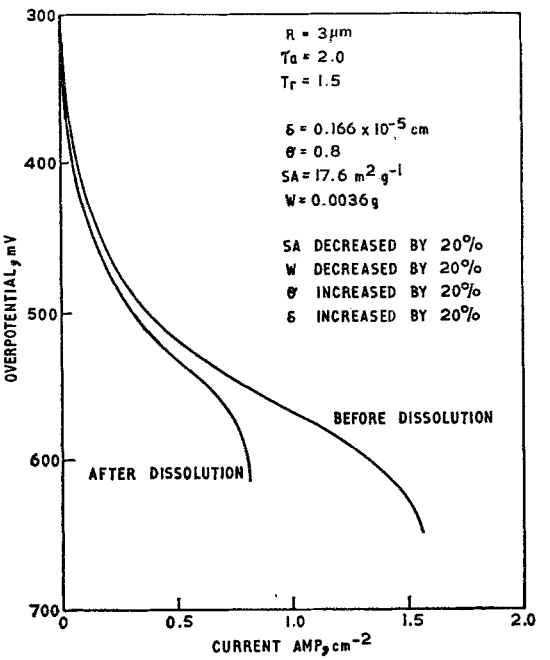

Fig. 11. The theoretical effect of platinum dissolution allowing for a decrease in surface area and loading and an increase in porosity and film thickness.

due to poisoning, platinum dissolution, or sintering of the catalyst during electrode fabrication is shown in Fig. 9. The relative decrease in performance increases with decreasing current density.

Fig. 10 shows a decay in performance due to platinum dissolution (20%) from the cathode (experiments have shown that this occurs in the operating potential range). It has been assumed that the platinum has dissolved out evenly from the agglomerates leading to a corresponding increase in porosity. The surface area has also been decreased by 20%. It is interesting that the overall decrease in performance is only about 15%. These surfaces areas (BET) and performance changes have also been verified experimentally.

The effect of the dissolution of 20% of the platinum is also shown in Fig. 11. In addition δ has been increased from $0{\cdot}87 \times 10^{-6}$ cm to $1{\cdot}66 \times 10^{-6}$ cm. The change in agglomerate radius is negligible. To some extent uniform platinum dissolution would be expected to increase the average value of θ. However, dissolution would be expected to be somewhat higher at the outside of the agglomerate, due to the slightly higher OH^- concentration. The most important effect, however, is penetration of the PTFE/gas phase by the electrolyte; it can be seen that as δ increases the performance suddenly decreases and the

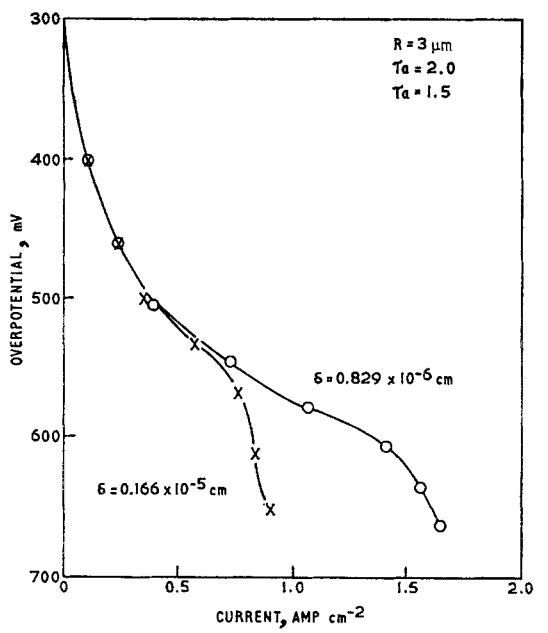

Fig. 12. The theoretical effect of increasing the film thickness i.e., a situation analogous to flooding of the electrode.

limiting current moves towards the fuel cell operating region.

Fig. 12 shows the effect of electrolyte penetration of the PTFE/gas phase without any other effects. Limiting current experiments on electrodes that have been allowed to soak in KOH for 1,000 h have shown that this phenomenon occurs. It is not known, however, whether the effect is primarily due to platinum dissolution or wetting of the PTFE particles.

Conclusions

The basic cylindrical agglomerate model has been improved and adapted for oxygen reduction at the Pt/PTFE/Ni fine pore electrode. Performance levels have been predicted. Bulk parameters (such as agglomerate radius, porosity and tortuosity) of the electrode structure can be determined by comparing theoretical current-voltage curves with IR-free experimental curves. The experimental curves, which vary with the electrode preparation procedure, are very similar to the theoretical curves and are for this reason not shown in the figures. Finally, the effect on electrode performance of different decay mechanisms has been predicted.

References

[1] R. de Levie, 'Advances in Electrochemistry and Electrochemical Engineering', **6**, p. 329, Wiley, Interscience, New York (1967).
[2] C. G. Austin and S. Almaula, *J. Electrochem. Soc.*, **114** (1967) 927.
[3] R. Brown, private communication.
[4] L. A. Horve, private communication.
[5] J. Giner and C. Hunter, *J. Electrochem. Soc.*, **116** (1969) 1124.

List of symbols

α	Transfer coefficient	
C	Concentration of O_2 in electrolyte	mol cm^{-3}
C_i	Concentration of O_2 at $r = R$	mol cm^{-3}
C_o	Concentration of O_2 in electrolyte at $r = \delta$	mol cm^{-3}
D_{O_2}	Diffusion coefficient of O_2 in KOH	cm^2 sec^{-1}
δ	Film thickness	cm
E	Overpotential of the electrode	V
F	Faraday's constant	
i	Electrode current density	A cm^{-2}
i_a	Current per agglomerate	A
$I_1(Z)$	First order Bessel function	
$I_0(Z)$	Zero order Bessel function	
j	Local current density	A cm^{-2}
j_0	Exchange current density	A cm^{-2}
L	Agglomerate length (catalyst thickness)	cm
N	Number of electrons in rate determining step	
N_a	Number of agglomerates per cm^2 of electrode	
ϕ	Potential drop along agglomerate	V
ϕ_L	Potential drop at $L\tau_a$	V
r	Radial direction	
R	Radius of agglomerate	cm
R_o	Gas constant	
ρ	Density of platinum	g cm^{-3}
S_g	Surface area per gram	cm^2 g^{-1}
S_{O_2}	Solubility coefficient of O_2	mol cm^{-3}
σ_m	Electrolyte conductivity	(ohm cm)$^{-1}$
T	Absolute temperature	°K
τ_a	Axial tortuosity	
θ	Porosity of platinum in the agglomerate	
τ_r	Radial tortuosity of the agglomerate	
W	Catalyst loading	g cm^{-2}
x	Axial direction	